

New approach for beneficiation of REE from apatites

Jaroslav Majka¹, Julia Sordyl^{1,2}, Maciej Manecki^{1,2}, Karin Högdahl¹

¹ *Department of Earth Sciences, Uppsala University, Uppsala, Sweden*

² *Department of Mineralogy, Petrography and Geochemistry, AGH University of Science and Technology, Krakow, Poland*

The objectives of the planned research and associated experiments were as follow:

- 1) To optimize the initially developed procedure for recovery of REE from apatite-bearing waste;
- 2) To develop the procedure for transformation of resulting precipitate into marketable product containing REE;
- 3) To optimize the details of experimental and analytical procedures of solids and solutions.

Based on tests and experiments conducted in 2020 (see our interim report), it was found that the most promising procedure of recovery of REE from apatite-bearing waste is the one using phosphoric acid. Briefly: dissolution in 30% P₂O₅, solid to liquid ratio = 1 g/10 ml, temperature: 25 °C; followed by precipitation of pyromorphite by the reaction with the solution containing Pb(NO₃)₂ and NaCl at pH between 2 and 3 maintained with 1M NaOH.

To address the objectives, the following specific tests were performed:

- I. Optimization of the procedure for dissolution in phosphoric acid.
- II. Optimization of the procedure for precipitation of REE-rich pyromorphite.
- III. Development of procedures for conversion of REE-rich pyromorphite into a marketable product.
- IV. Syntheses of pure pyromorphite containing REE.
- V. Optimization of methodology for analysis of REE content in solids and solutions using ICP-MS.
- VI. Final development of the technology.

I. Optimization of the procedure for dissolution in phosphoric acid

The leaching experiment in H₃PO₄ was repeated in triplicate (sample A, B, and C). Three aliquots of solid of 5 g each were poured into 50 ml of 30% P₂O₅ solution and left for leaching at 25°C (stirring continuously). The solutions were sampled after 24 hours and after 48 hours. Table 1 shows the results obtained using ICP analysis.

Table 1. ICP-MS analysis of solutions (triplicate) after 24 hours and 48 hours of leaching in H₃PO₄.

Element	Concentrations after 24 hours of leaching [mg/L]						Concentrations after 48 hours of leaching [mg/L]						% increase after 48h
	Sample A	Sample B	Sample C	Average	Standard dev.	% Standard dev.	Sample A	Sample B	Sample C	Average	Standard dev.	% Standard dev.	
Sc	0.0845	0.0719	0.0927	0.083	0.01	12.6	0.1283	0.1354	0.1384	0.134	0.01	3.9	61
Y	3.9603	3.6236	4.335	3.973	0.36	9.0	4.3624	4.255	4.1322	4.250	0.12	2.7	7
La	2.1177	2.0211	2.3131	2.151	0.15	6.9	3.3095	3.4544	3.2362	3.333	0.11	3.3	55
Ce	4.5931	4.3589	5.0689	4.674	0.36	7.7	6.7206	7.0076	6.6035	6.777	0.21	3.1	45
Pr	0.5878	0.5542	0.6411	0.594	0.04	7.4	0.8089	0.8222	0.7877	0.806	0.02	2.2	36
Nd	3.2474	3.1353	3.5731	3.319	0.23	6.9	4.4959	4.6461	4.324	4.489	0.16	3.6	35
Sm	0.6828	0.645	0.7464	0.691	0.05	7.4	0.7977	0.805	0.7662	0.790	0.02	2.6	14
Eu	0.1846	0.1735	0.2012	0.186	0.01	7.5	0.2097	0.2087	0.1944	0.204	0.01	4.2	10
Gd	0.7459	0.6925	0.8328	0.757	0.07	9.4	0.8289	0.8214	0.7893	0.813	0.02	2.6	7
Tb	0.1053	0.0989	0.1162	0.107	0.01	8.2	0.1171	0.1144	0.1087	0.113	0.00	3.8	6
Dy	0.6586	0.6187	0.7267	0.668	0.05	8.2	0.7153	0.7098	0.6805	0.702	0.02	2.7	5
Ho	0.1363	0.1282	0.1519	0.139	0.01	8.7	0.1497	0.146	0.1405	0.145	0.00	3.2	5
Er	0.38	0.3539	0.4211	0.385	0.03	8.8	0.4147	0.3963	0.3882	0.400	0.01	3.4	4
Tm	0.0515	0.0485	0.0585	0.053	0.01	9.7	0.0571	0.0556	0.0544	0.056	0.00	2.4	5
Yb	0.3203	0.2922	0.3594	0.324	0.03	10.4	0.3438	0.3344	0.3338	0.337	0.01	1.7	4
Lu	0.0442	0.0405	0.0489	0.045	0.00	9.5	0.0481	0.0473	0.0461	0.047	0.00	2.1	6
Th	0.3373	0.3212	0.4259	0.361	0.06	15.6	0.3557	0.3798	0.4276	0.388	0.04	9.4	7

Conclusions:

A higher REE content was found after 48 hours of leaching: the averages after 48 hours were higher than the averages after 24 hours by from 5 to 61 relative percent of the 24 hours average. A higher repeatability between triplicates was found after 48 hours of leaching (lower standard deviation of the averages). Therefore, the 48 hours leaching is accepted as the optimum time to dissolve all apatites under these conditions.

II. Optimization of the procedure for precipitation of REE-rich pyromorphite

To increase the concentration of REE initially dispersed in the Ca-apatites present in the waste, a series of experiments testing different precipitation conditions were performed.

Table 2. Summary of experimental conditions varied in the experiments for optimization of precipitation processes

Exp. 1	A solution of 0.3M Pb(NO ₃) ₂ and 0.06M NaCl was prepared by dissolving Pb(NO ₃) ₂ and NaCl in double-distilled water and then the leaching solution was added by dropwise. The pH was maintained at 2 - 3 with 1M NaOH throughout the whole experiment.
Exp. 2	The pH of leaching solution was slowly raised with 12M NaOH to 1.5 and then the solution of 0.07M Pb(NO ₃) ₂ and 0.015M NaCl was added by dropwise. The pH was maintained at 2 - 3 with 1M NaOH throughout the whole experiment.
Exp. 3	The solution of 0.07M Pb(NO ₃) ₂ and 0.015M NaCl and leaching solution were both added by dropwise to the redistilled water. The pH was maintained at 2 - 3 with 1M NaOH throughout the whole experiment.

Results:

Exp. 1: The synthesis produced homogeneous, white crystalline powder. Both XRD (Figure 1) and semi-quantitative EDS analysis (Figure 3) indicated that the synthesized products were crystalline analogues of Pb-apatite. The micro-aggregates of crystals were spherical (Figure 2). No other phases were detected at the detection limit of the methods. ICP-MS analysis of the solution indicated that almost all REE were extracted from the solution and immobilized in the solid precipitate (Table 3).

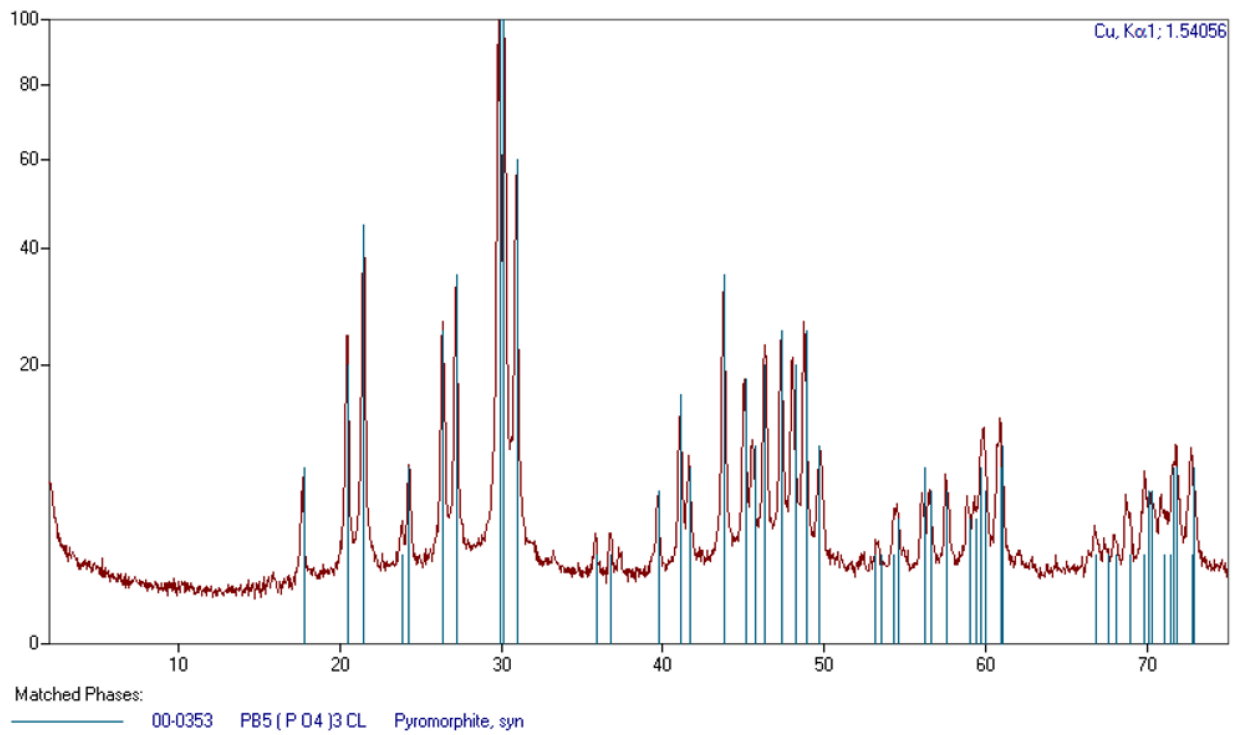


Figure 1. X-ray diffraction pattern of the powder synthesized in the experiment 1. The positions of all diffraction peaks correspond to pyromorphite $Pb_5(PO_4)_3Cl$.

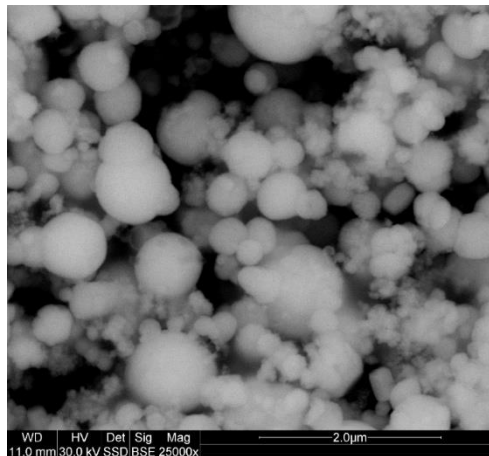


Figure 2. Scanning electron micrograph of the pyromorphite synthesized in the Exp. 1.

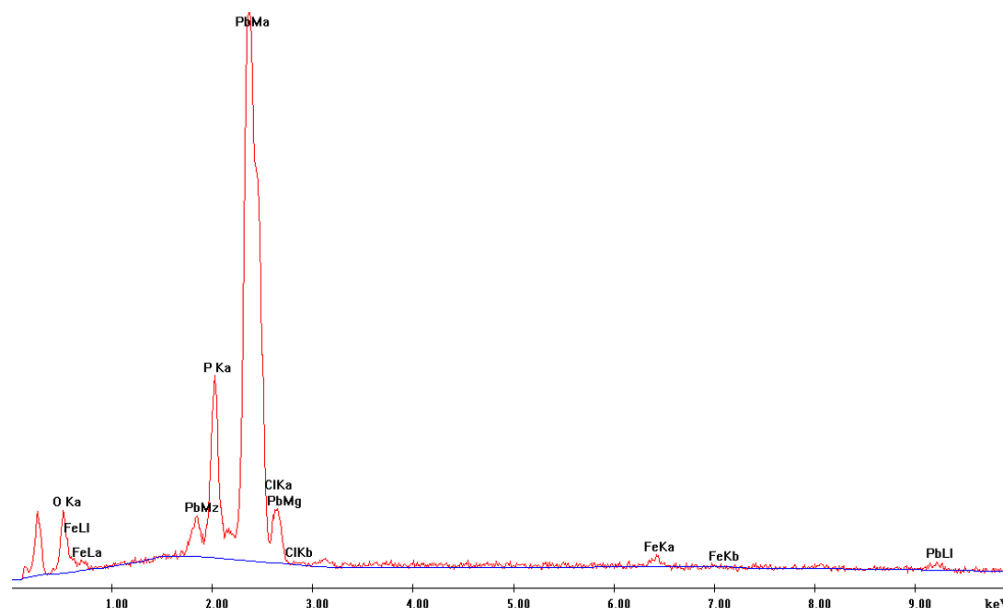


Figure 3. Elemental composition revealed by SEM/EDS analysis of the pyromorphite synthesized in the experiment 1: Pb, P, O and Cl are the major components, small admixture of Fe is apparent. REE are below the detection limit of the method.

Table 3. REE concentration in the solutions before and after precipitation of pyromorphite (results of ICP-MS analysis). The concentrations of REE after precipitation decreased significantly. This indicates that the REE were removed from the solution by crystallization of pyromorphite.

	Concentrations before precipitation (in leaching solution)	Concentrations after pyromorphite precipitation
	[mg/L]	
Sc	0.1283	0.0011
Y	4.3624	0.0227
La	3.3095	0.0035
Ce	6.7206	0.0055
Pr	0.8089	<0.001
Nd	4.4958	0.0049
Sm	0.7977	0.0015
Eu	0.2096	<0.001
Gd	0.8288	0.0027
Tb	0.1170	<0.001
Dy	0.715	0.0022
Ho	0.1497	<0.001
Er	0.4147	0.0013
Tm	0.0571	<0.001
Yb	0.3438	0.0010
Lu	0.0481	<0.001
Th	0.3556	<0.001

Conclusion: At the conditions of the experiment pyromorphite is the only crystallized phase. The recovery of REE is close to 100%. However, due to the use of a large amount of lead for complete reaction, a large amount of pyromorphite precipitates: larger mass of solids is produced than processed. As a result, the REE elements are more dispersed in solid product than they were in the initial waste. This causes the REE to be more dispersed (rather than to be concentrated) in the product than in the initial Ca-apatite. All REE are contained in the single phase though.

Exp. 2: SEM/EDS analysis revealed the presence of two distinct phases (Figure 4). Pyromorphites up to 5 micrometers in size were found together with aggregates of very fine crystals of markedly different composition. EDS of both phases are shown in Figure 5. The phase that formed beyond the pyromorphite is probably an aluminum-iron phosphate containing REE that formed in the early stage of the synthesis when the pH in the leaching solution was raised. However, XRD analysis showed no phase other than pyromorphite (Figure 6), indicating that the phosphate phase was not crystalline.

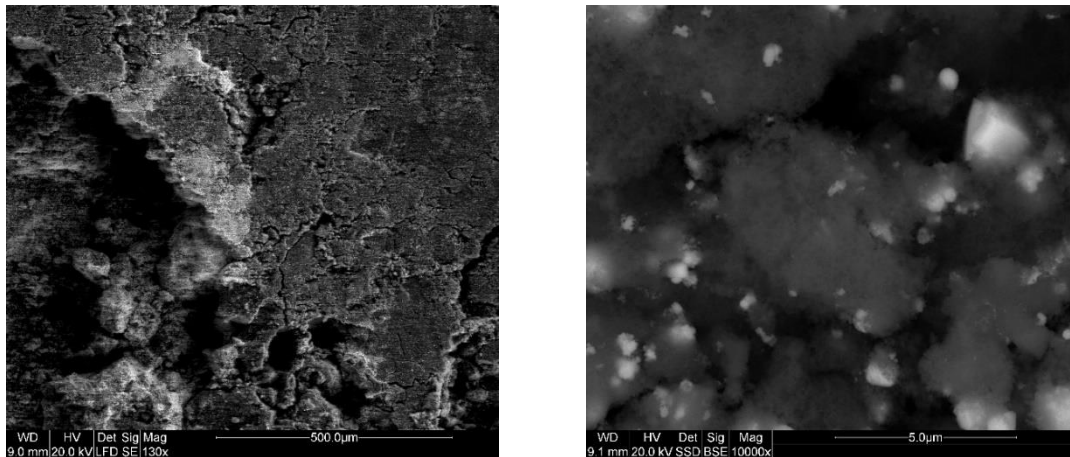


Figure 4. Scanning electron micrographs of the powder synthesized in the experiment 2. The left panel shows that the powder consists of only 20% pyromorphite (white crystals) and 80% other phase (dark mass). The right panel is a close-up and reveals the lack of crystallinity of the phase.

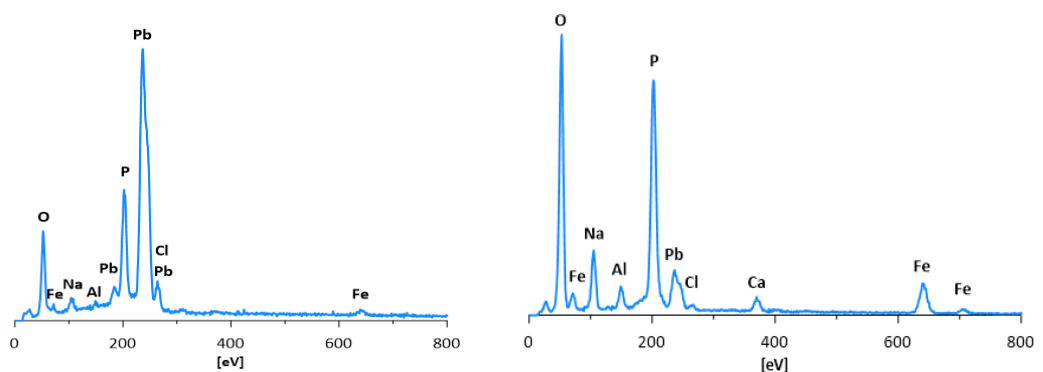


Figure 5. EDS of the pyromorphite (left) and aluminum-iron phosphate (right) precipitated in experiment 2. REE are not detected in any of them due to the detection limit of the method.

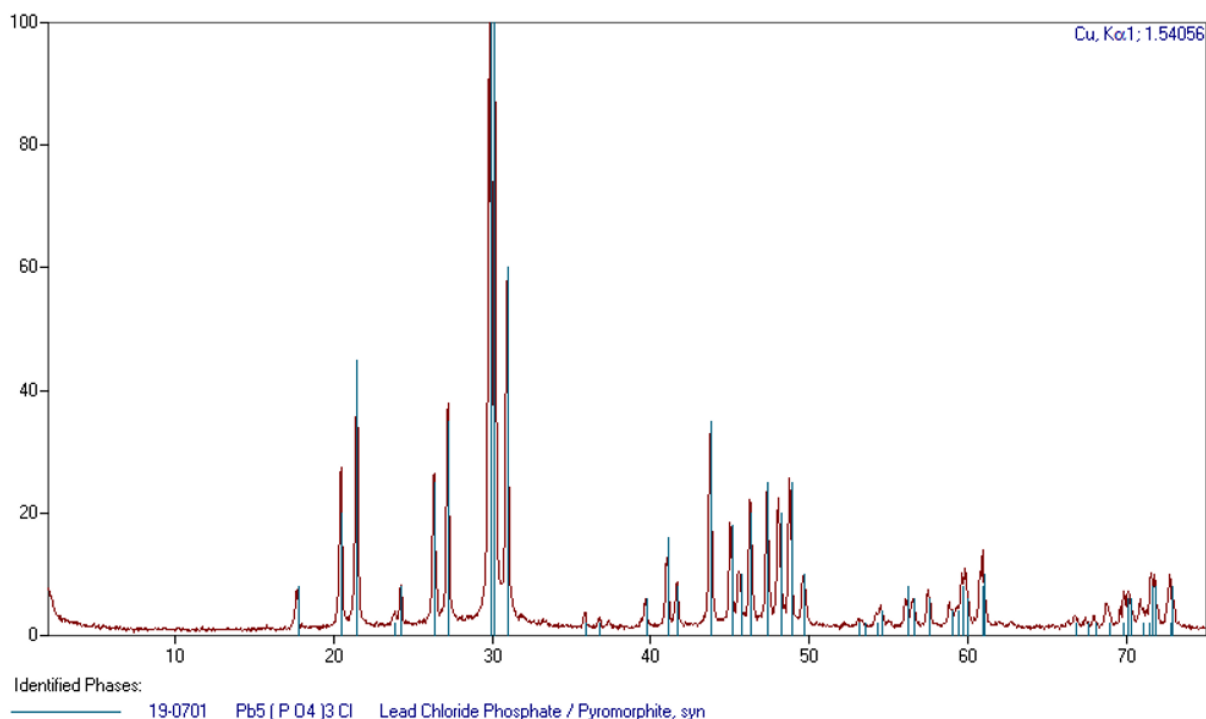


Figure 6. X-ray diffraction pattern of the powder synthesized in the experiment 2. The positions of diffraction peaks of synthesized powder correspond to pyromorphite. No other phases were detected which means lack of crystallinity of the other components of the precipitate apparent in SEM images.

Exp. 3: The results are identical to Experiment 2. SEM/EDS analysis showed the presence of two distinct phases (Figure 7). However, for this experiment, the pyromorphite crystals were smaller ($< 1 \mu\text{m}$). Phosphate aggregates were also visible. Due to the very small size of the pyromorphite crystals, it was not possible to perform distinct EDS analyses of the two phases. The presented EDS spectrum is a mixture of the composition of both phases (Figure 8).

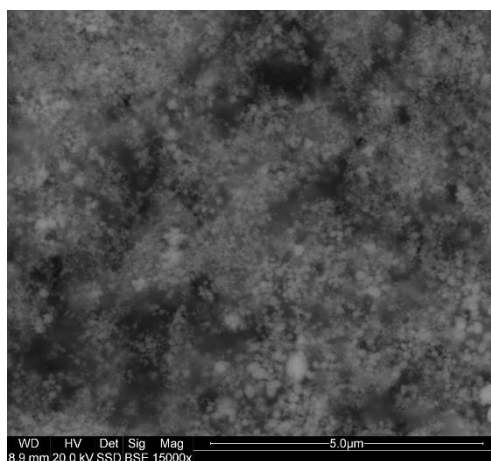


Figure 7. Scanning electron micrographs of the powder synthesized in the experiment 3. Powder consists of small pyromorphite crystals and shapeless (probably non-crystalline) phosphate mass.

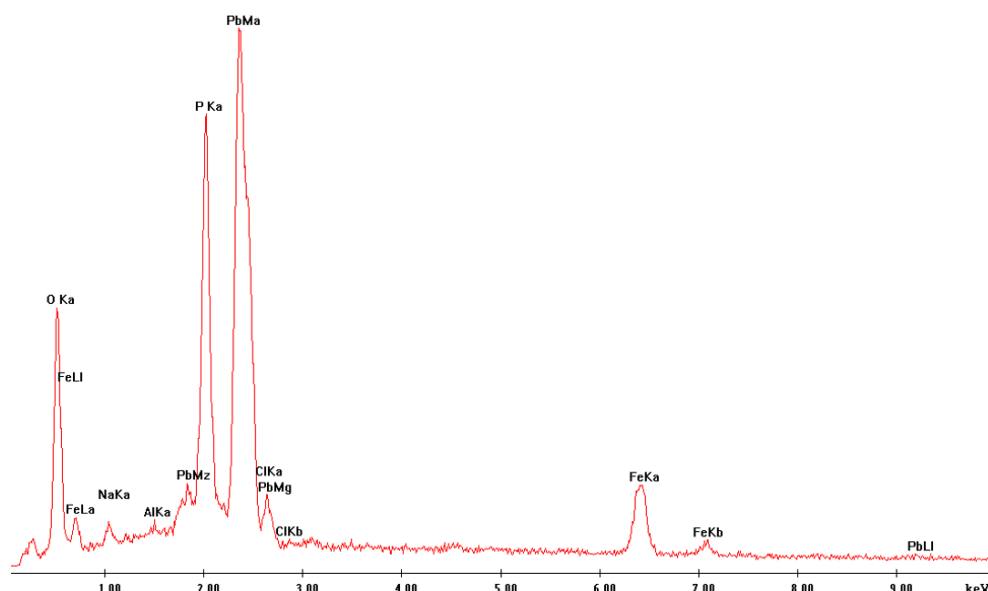


Figure 8. EDS spectrum of the pyromorphite and aluminum-iron phosphate precipitated in experiment 3. REE are not detected due to the content below the detection limit.

Conclusion:

Attempts to optimize PY precipitation conditions for obtaining a smaller amount of PY more enriched in REE were not successful. After changing the conditions, the undesirable phenomenon of REE phosphate co-precipitation occurred. The REE phosphates were of low crystallinity, very small particle size and ambiguous chemical composition. Such components may hinder the separation of precipitate from solution in the future and may be a source of REE loss throughout the procedure.

III. Development of procedures for conversion of REE-rich pyromorphite into a marketable product.

In view of the results of the previous experiments, an alternative avenue of research was adopted to optimize the procedures. Instead of aiming to obtain a small amount of pyromorphite highly enriched in REE, the focus was placed on complete removal (recovery) of REE from solutions. This is to minimize potential sources of REE loss as much as possible. This is favored by the completeness of REE removal from aqueous solutions by precipitation of REE-rich crystalline pyromorphite found in previous experiments provided that no other REE-bearing phases are formed.

Therefore, it was accepted that REE-rich pyromorphite is an intermediate product resulting from a certain stage of the whole technology, and it is necessary to develop the methods of its processing to obtain a commercial product rich in REE. Currently, REE-rich pyromorphite, which is a new material developed in this research project. It is not known worldwide and it is not considered as a

commercial product. The examples of commercial products are REE sulfates or REE oxalates. Therefore, two chemical reaction routes were tested to separate Pb from REE: one by transformation to sulfates and the other by transformation to oxalates, namely:

- reaction of REE-rich pyromorphite with sulfuric acid;
- reaction of REE-rich pyromorphite with oxalic acid.

This technological path is founded on the following assumptions:

- Sulphates and oxalates of Pb and REE have low solubility, but their solubility differs from each other;
- REE are not incorporated into the structure of crystallizing Pb sulfates or oxalates but they form their own distinct phases.

A series of experiments was performed using 0.5 g of the synthetic REE-enriched pyromorphite reacted with aqueous solutions of 0.5 M and 1 M oxalic acid or 1.25 M, 2.5 M, and 5 M sulphuric acid. After 24 hours the reaction, products were centrifuged, washed, dried, and analysed using scanning electron microscopy with energy dispersive spectroscopy (SEM-EDS) and powder X-ray diffraction (XRD). The solutions were analysed using inductively coupled plasma mass spectrometry (ICP-MS).

Reaction of REE-enriched pyromorphite with sulphuric acid resulted in complete transformation into lead sulphate PbSO_4 , as indicated by XRD (Figure 9). The precipitate formed aggregates of thin, rhomboidal, tabular crystals, up to 5 μm in size (Figure 10). The volume of the unit cell, refined in the orthorhombic system, was larger by 2.72 \AA^3 than the unit cell of pure lead sulphate. This is probably caused by the REE incorporation into the structure of lead sulphate. Analysis of the solution in which the transformation experiment was performed showed that 85% of the REE initially present in pyromorphite was coprecipitated with Pb in the form of PbSO_4 while only 15 % went into solution.

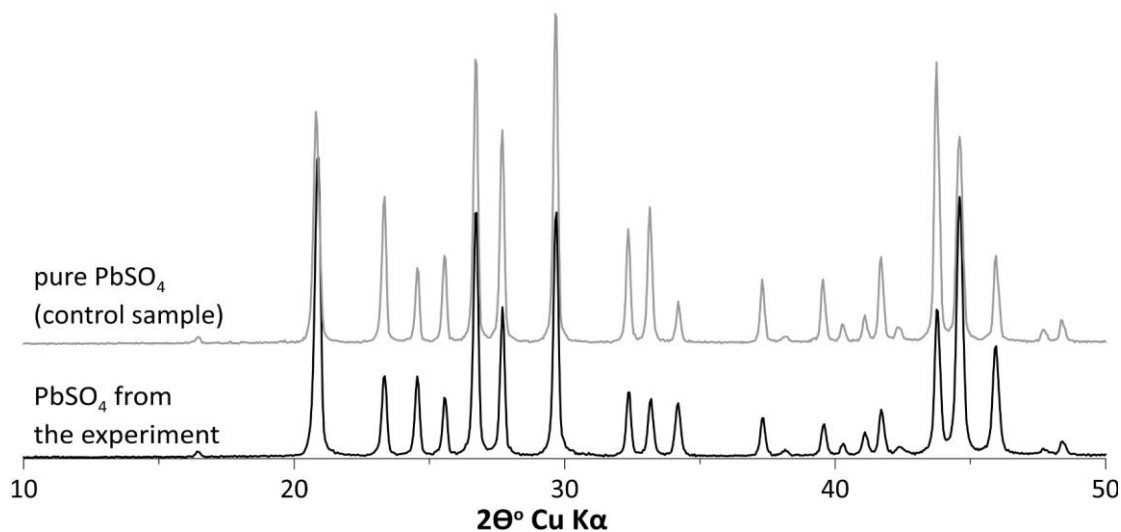


Figure 9. Comparison of diffraction patterns of the powder resulted from transformation of REE-rich pyromorphite in sulfuric acid (lower) with a control sample (upper). The positions of all diffraction peaks correspond to lead sulphate, no other phases were detected.

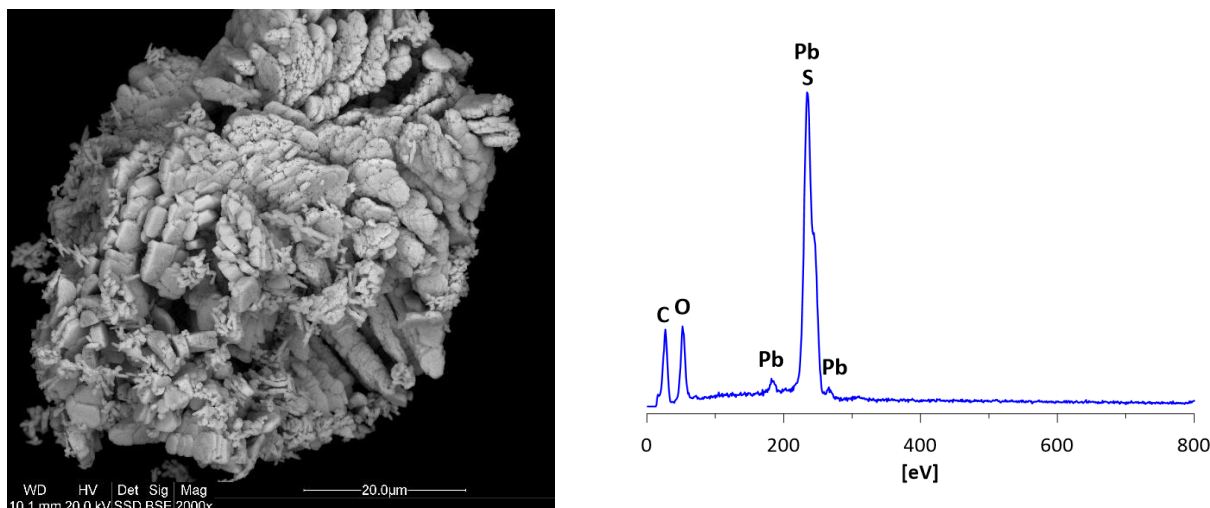


Figure 10. Scanning electron micrograph and EDS elemental analysis of PbSO_4 resulted from the transformation of pyromorphite in sulfuric acid. REE are below the detection limit.

In the experiments with oxalic acid, complete dissolution of REE-enriched pyromorphite resulted in formation of two distinct, crystalline phases: lead (II) oxalate and REE oxalate (Figure 11). SEM images showed thin, needle-like crystals of PbC_2O_4 , 10-20 μm in size, and tabular crystals of $\text{REE}_2(\text{C}_2\text{O}_4)_3$ measuring up to 30 μm (Figure 12, 13). Unit cell volume of precipitated lead oxalate, calculated in the triclinic system, was 185.37 \AA^3 , which is identical to pure lead oxalate. This indicated that REE did not incorporate into the lead oxalate structure. This remains to be confirmed by chemical microanalysis.

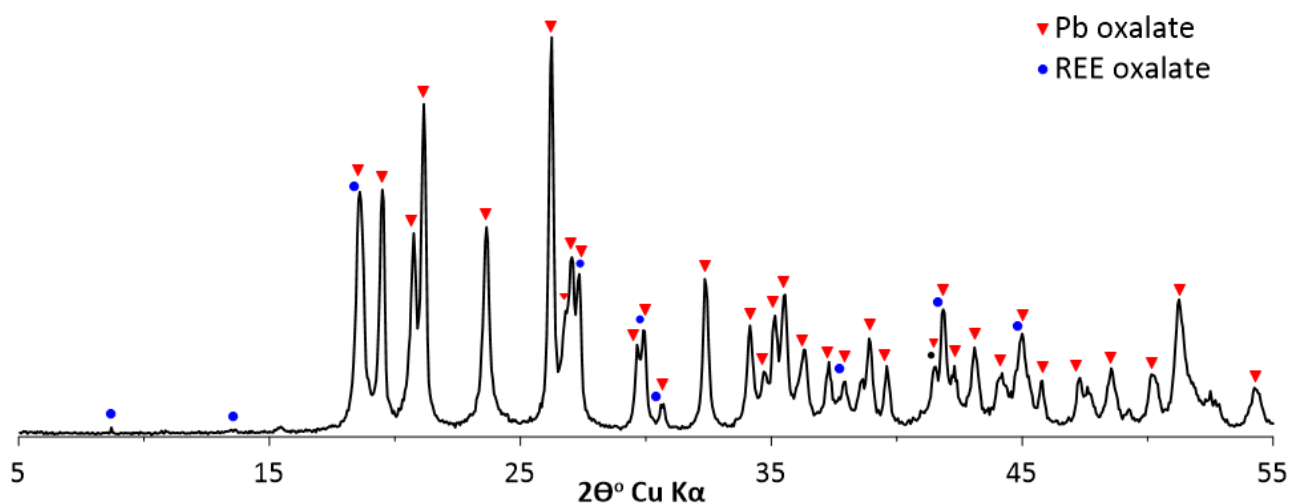


Figure 11. X-ray diffraction pattern of the powder resulting from the reaction of REE-rich pyromorphite with oxalic acid. The positions of diffraction peaks indicate that all REE-rich pyromorphite was converted into a mixture of Pb oxalate and REE oxalate.

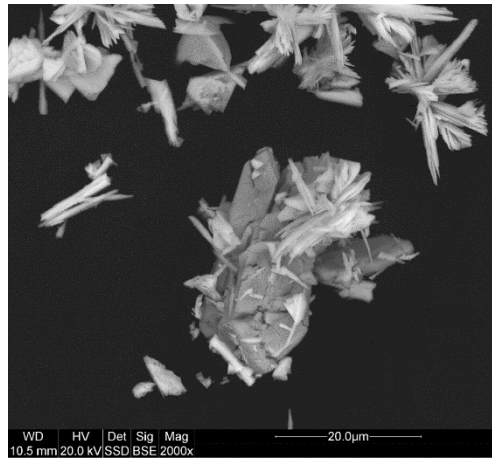


Figure 12. Scanning electron micrograph of REE oxalate (tabular crystals) and Pb oxalate (needles) resulting from the reaction of pyromorphite with oxalic acid.

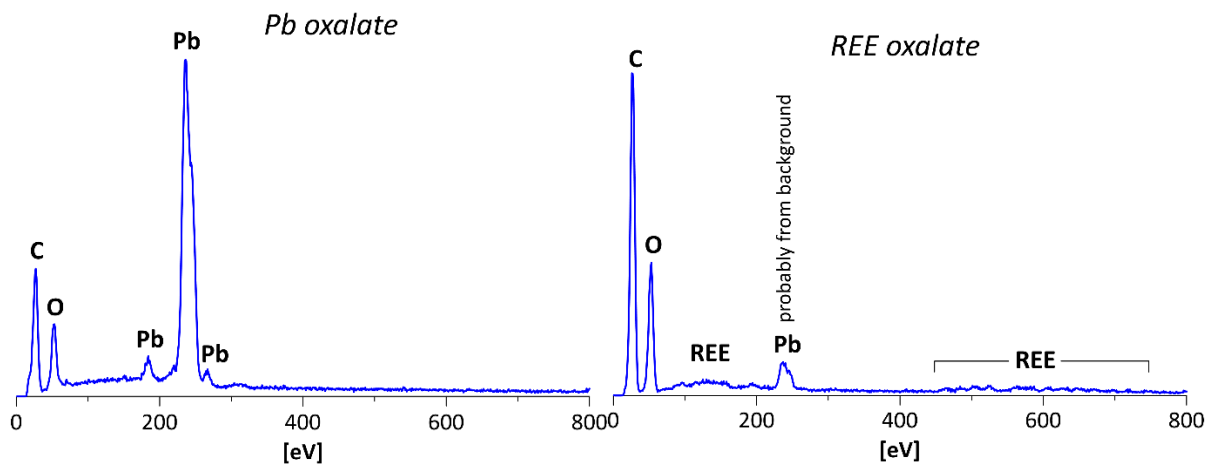


Figure 13. EDS elemental analysis of Pb oxalate (left) and REE oxalate (right) resulting from the transformation of pyromorphite in oxalic acid.

Conclusions:

The preliminary results obtained from the experiments indicate that the direction of research chosen is correct and the performance of the procedures tested is promising. The best results will probably be obtained by appropriate sequential combination of both methods: precipitation of Pb sulfate followed by reaction with oxalate. This avenue will be further investigated in the future.

IV. Syntheses of pure pyromorphite containing REE

A series of experiments was conducted to:

- determine if REE fractionation occurs upon coprecipitation with pyromorphite, which could be a source of losses in the future;
- determine the maximum amount of REE which can be absorbed by crystallizing pyromorphite;

- compare the degree of incorporation of individual REEs into the structure of pyromorphite crystallizing from aqueous solutions.

Synthetic analogue of REE-rich pyromorphite was precipitated from aqueous solutions (Figure 14) using $\text{Pb}(\text{NO}_3)_2$, $\text{NaH}_2\text{PO}_4 \cdot \text{H}_2\text{O}$, NaCl and a mixture of REE and Th in HNO_3 (100 mg/L standard solution, VHG, USA). In control experiment no REE were used. The synthesis was carried out at ambient conditions at $\text{pH} = 3$ (HNO_3 , NaOH). The initial concentration of each REE and Th equaled to 100 mg/L. The precipitate was characterized using scanning electron microscopy with energy dispersive spectroscopy (SEM-EDS), powder X-ray diffraction (XRD), infrared absorption spectroscopy (FTIR), and Raman microspectroscopy. In addition, the concentration of the REE incorporated into the pyromorphite structure was determined by wet chemical analysis of the product (dissolved in 6M HNO_3) using inductively coupled plasma mass spectrometry (ICP-MS).

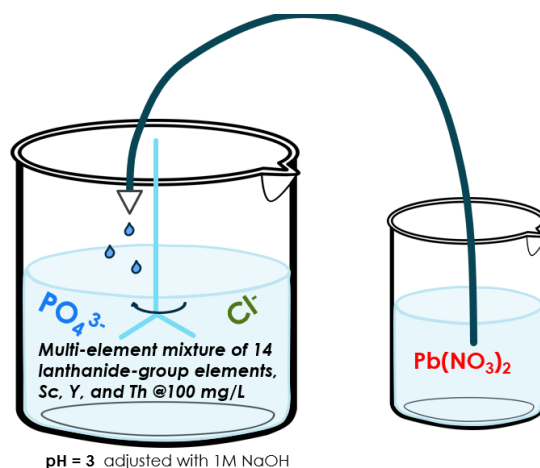


Figure 14. Experimental setup of a synthesis of REE-rich pyromorphite

The synthesis resulted in precipitation of a white powder. Comparison of X-ray diffraction pattern with the result of control experiment indicates that the positions of all diffraction peaks of synthesized powder correspond to pyromorphite (Figure 15). No other phases were detected. The crystals were 1 to 3 μm in size. They formed aggregates of elongated, slightly rounded rods resembling pyromorphite synthesized in the absence of REE (Figure 16). All the methods used revealed the absence of components other than the intended REE-rich pyromorphite. Unit cell parameters, refined in hexagonal system, were identical to pure pyromorphite: $a = 9.9996 \text{ \AA}$, $c = 7.3192 \text{ \AA}$, $V = 633.82 \text{ \AA}^3$. Wet chemical analysis indicated that the precipitate contained 10 wt.% of all REE and Th combined. Most of the REE were incorporated at the same level (showing little or no fractionation of light or heavy REE) except for Sc and Th, which were preferentially scavenged from the solution: their content in the pyromorphite was two times higher than that of the other REE. Pyromorphite may contain more REE and Th than other apatites due to its larger unit cell. This is probably also the reason for a weaker fractionation.

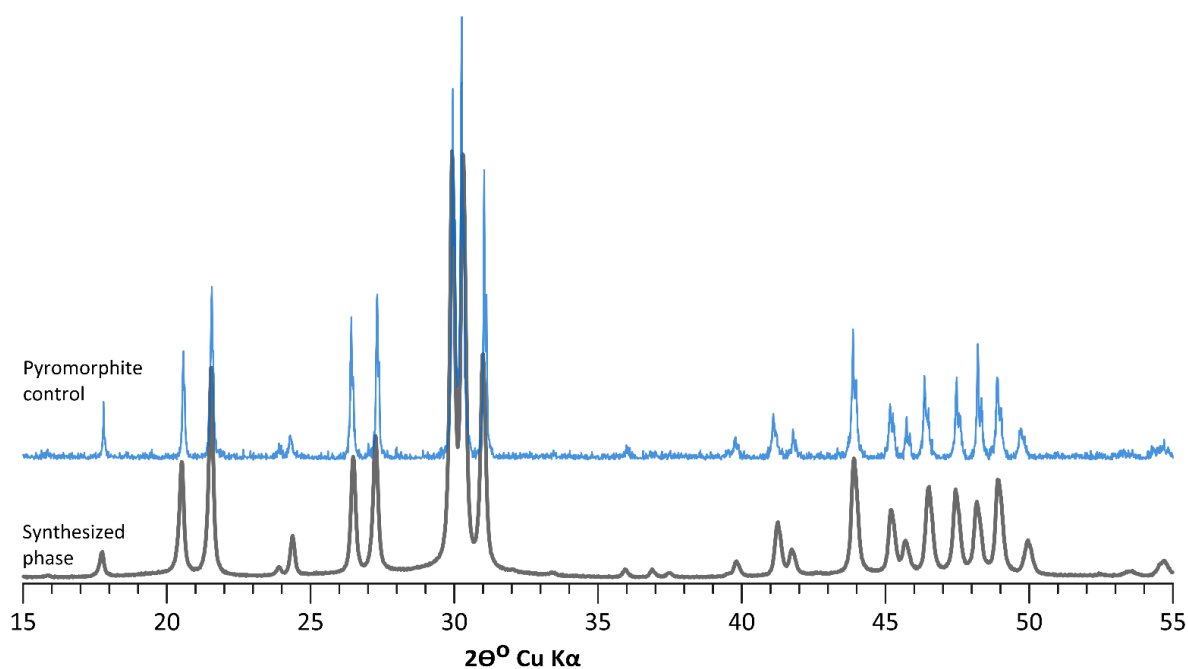


Figure 15. Comparison of diffraction patterns of the synthesized REE-rich pyromorphite (lower) and control sample (upper). The position of diffraction all peaks corresponds to pyromorphite. No other phases were detected.

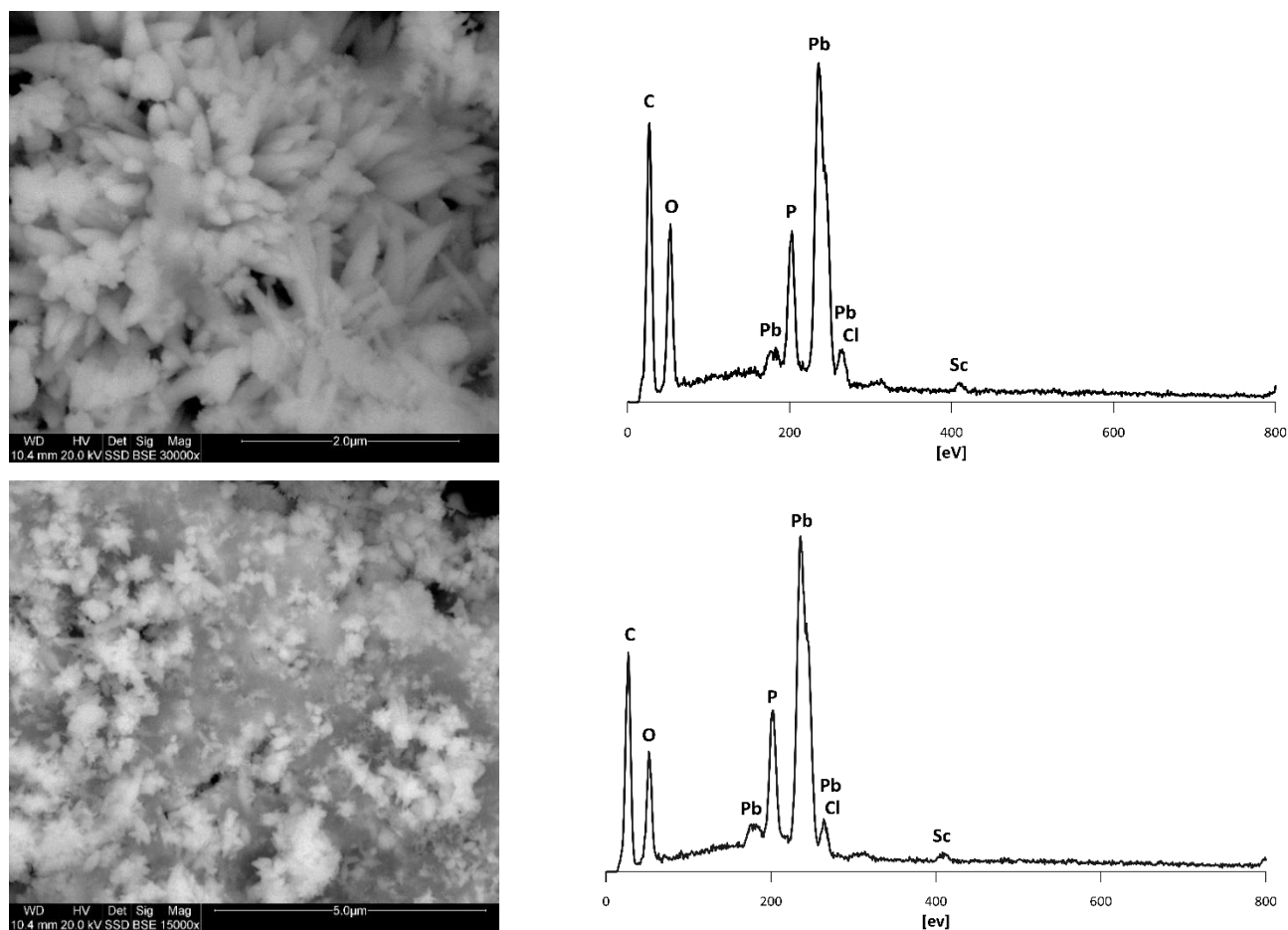


Figure 16. Scanning electron micrographs and EDS analyses of synthetic REE-rich pyromorphite. SEM images revealed small amounts of very fine grain substance (lower image). EDS spectra, however, did not reveal differences in chemical composition.

Table 4. ICP-MS analysis of solutions before and after precipitation of pyromorphite and calculated % of removal of each single REE.

	Concentration before precipitation [mg/L]	Concentration after precipitation [mg/L]	% of removal
Sc	81.08	<0.001	100
Y	81.08	32.72	60
La	81.08	35.17	57
Ce	81.08	28.55	65
Pr	81.08	26.57	67
Nd	81.08	26.11	68
Sm	81.08	20.44	75
Eu	81.08	25.64	68
Gd	81.08	27.65	66
Tb	81.08	27.59	66
Dy	81.08	28.39	65
Ho	81.08	30.34	63
Er	81.08	30.90	62
Tm	81.08	30.88	62
Yb	81.08	30.51	62
Lu	81.08	35.53	56
Th	81.08	<0.001	100

Table 5. Content of REE (wt% and ppm) absorbed by pyromorphite, based on wet chemical analysis using ICP-MS. Most of the REE were incorporated at the same level (showing little fractionation of light vs heavy REE) except for Sc and Th.

Element	Wt%	ppm
Sc	0.69	6918
Y	0.33	3270
La	0.36	3604
Ce	0.49	4882
Pr	0.54	5383
Nd	0.41	4062
Sm	0.43	4304
Eu	0.42	4214
Gd	0.37	3735
Tb	0.45	4457
Dy	0.38	3760
Ho	0.41	4095
Er	0.34	3394
Tm	0.40	3975
Yb	0.33	3333
Lu	0.36	3641
Th	0.69	6895
Σ	7.39	

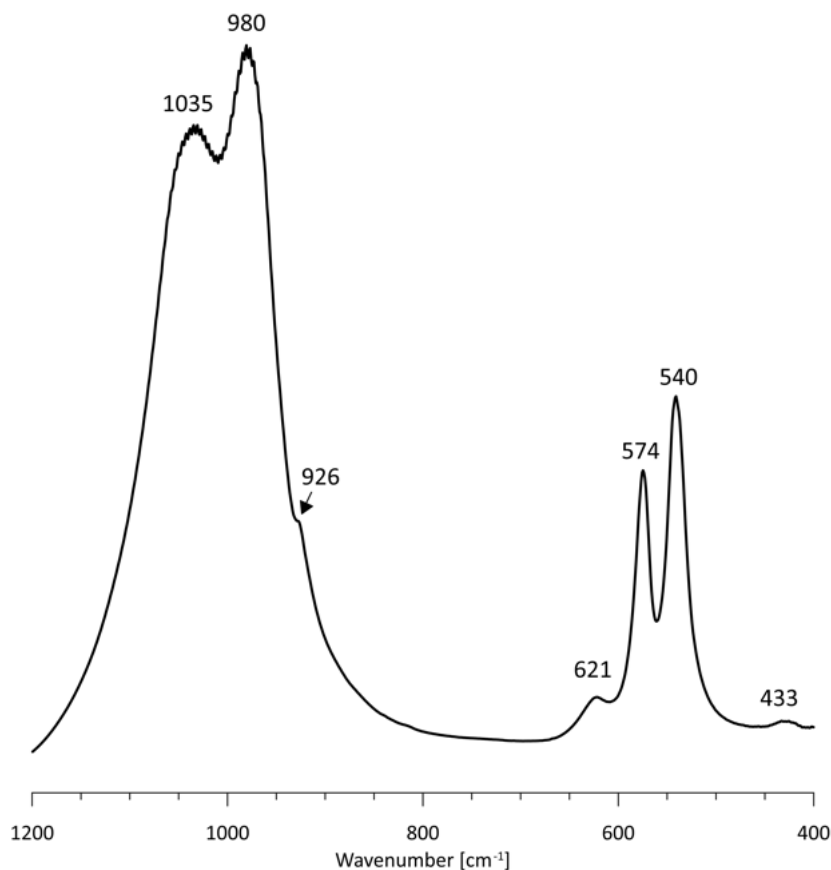


Figure 17. Infrared spectra of REE-rich pyromorphite in the low wavenumber region of PO₄ vibrations. No differences were observed between REE-rich pyromorphite and pure pyromorphite.

To compare the incorporation processes of selected individual REE into the structure of pyromorphite crystallizing from aqueous solutions, four syntheses were carried out to obtain La-, Sm-, Y-, and Pr-rich pyromorphite. Precipitation experiments from aqueous solution were carried out using the same experimental setup and the following reagents: Pb(NO₃)₂, NaH₂PO₄·xH₂O, NaCl and one of the following: La(NO₃)₃ · x 6H₂O, Sm(NO₃)₃ · x 6H₂O, Y(NO₃)₃ · x 6H₂O and Pr(NO₃)₃ · x 6H₂O. The first attempts were unsuccessful due to co-precipitation of REE-phosphates. Therefore, the precipitation methodology needs more work and improvements. It is currently under development. Figure 18 shows SEM images of the precipitated phases.

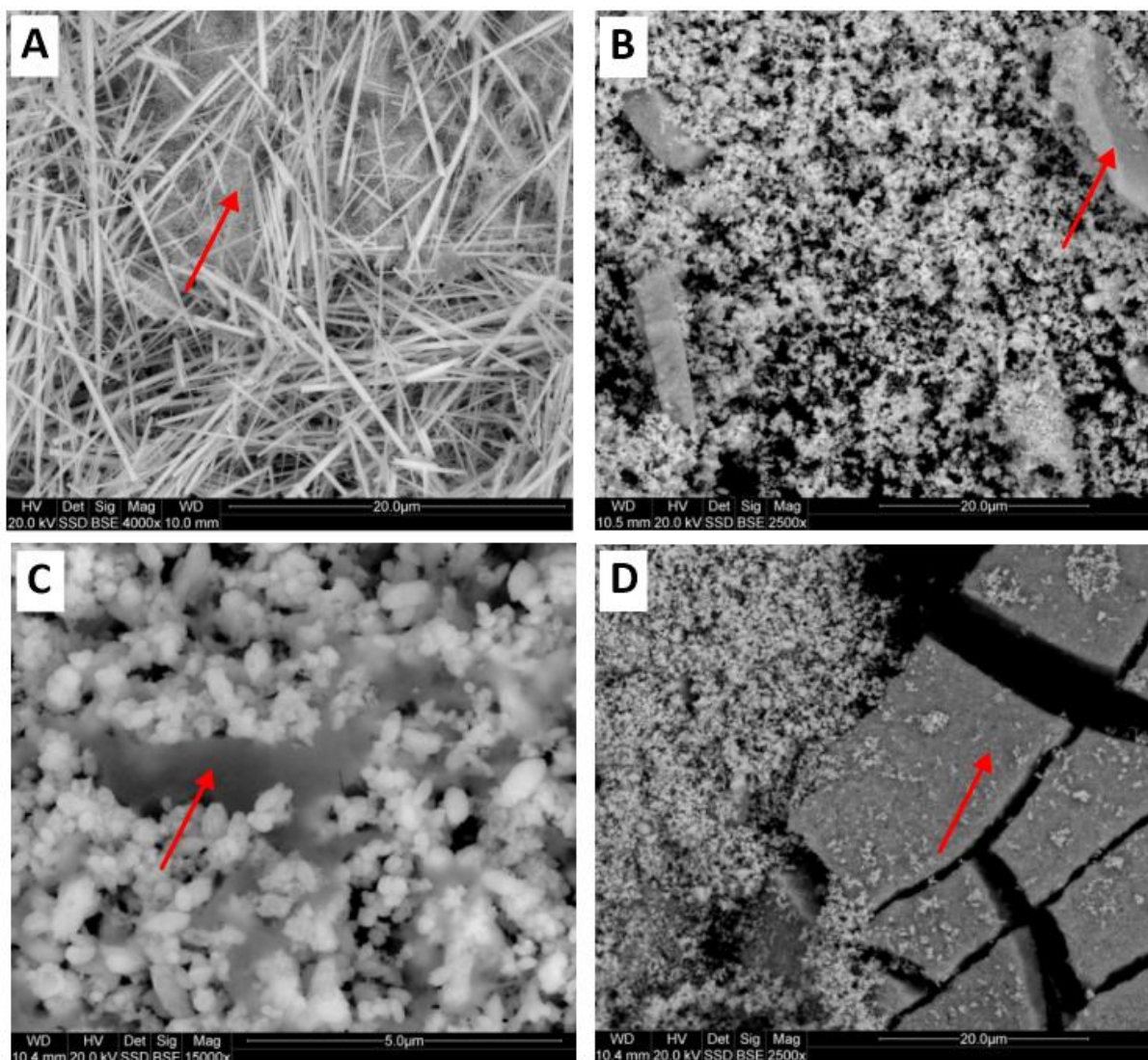


Figure 18. Scanning electron micrographs of synthesized powders: La-pyromorphite (A), Sm-pyromorphite (B), Y-pyromorphite (C), Pr-pyromorphite (D). Red arrows point the unwanted phases coprecipitated.

V. Optimization of methodology for analysis of REE content in solids and solutions using ICP-MS

During the course of experiments and analyses, it was found that precise analysis of REE content in media with such complex matrices as solids and solutions under study is often problematic, partly due to chemical coincidences and partly due to physical properties of concentrated solutions (viscosity, rapid wear of spectrometer parts). Therefore, several experiments were performed under well-defined conditions and with known chemical compositions of solids and solutions which allowed recovery to be calculated. Some imperfections in the analyses were identified. Determination of solution concentrations after dissolution of pyromorphite in a mixture of EDTA+HNO₃ was problematic. Also, inconsistencies were found in the case of Sc and Th determinations. Therefore, a new procedure for "wet" chemical analyses of precipitates and other solids without EDTA was

developed. REE reference materials are also currently being analyzed for optimization of chemical analyses and REE determinations using ICP-MS.

VI. Final development of the technology

As a result of two years of work, the following technology was developed for recovery of REE from apatite-bearing waste resulting from processing of Kiruna-type iron ore (Figure 19). Repeatedly tested in the laboratory, the procedure has given positive results and is ready for upscaling. All the results indicate that the project was successful. A new, highly effective technology for the recovery of REE from waste has been developed using procedures and materials that have never been used for this purpose before. In addition, an important component of the developed technology, the technique for removing REE from aqueous solutions by precipitation of pyromorphite, is extremely efficient and appears to be versatile for use in other industrial technologies as well.

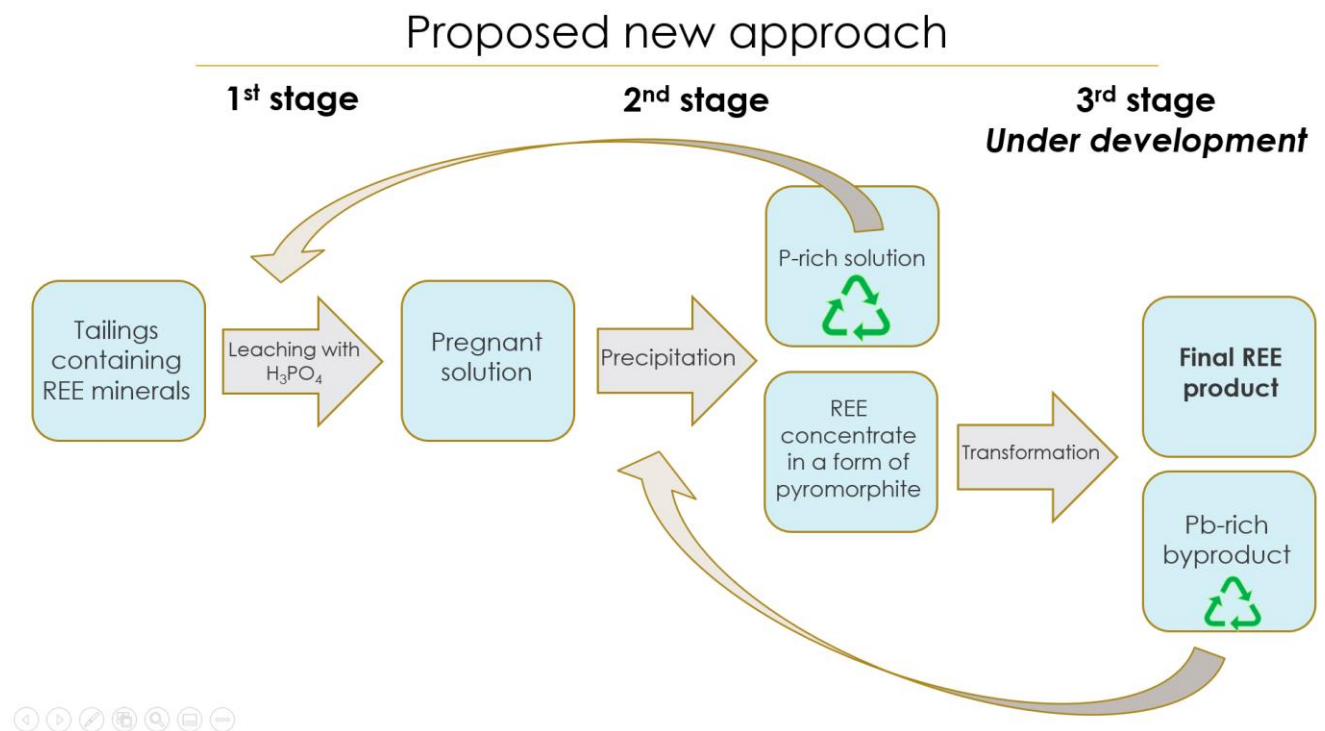


Figure 19. Proposed 3-steps technology of REE recovery from apatite-bearing waste.